Quantum Limited Superresolution of an Incoherent Source Pair in Three Dimensions

Zhixian Yu and Sudhakar Prasad*
Department of Physics and Astronomy, University of New Mexico, Albuquerque, New Mexico 87131, USA

(Received 26 May 2018; published 31 October 2018)

The error in estimating the separation of a pair of incoherent sources from radiation emitted by them and subsequently captured by an imager is fundamentally bounded below by the inverse of the corresponding quantum Fisher information (QFI) matrix. We calculate the QFI for estimating the full three-dimensional pair separation vector, extending previous work on pair separation in one and two dimensions. We also show that the pair-separation QFI is, in fact, identical to source localization QFI, which underscores the fundamental importance of photon-state localization in determining the ultimate estimation-theoretic bound for both problems. We also propose general coherent-projection bases that can attain the QFI in two special cases. We present simulations of an approximate experimental realization of such quantum limited pair superresolution using the Zernike basis, confirming the achievability of the QFI bounds.

DOI: 10.1103/PhysRevLett.121.180504

Rayleigh's pair-resolution criterion [1] is routinely superseded by modern imaging systems. An approach that entirely circumvents it employs PSF fitting and localization of single fluorescent molecules by selective excitation in which two closeby molecules are rarely, if ever, excited simultaneously [2–4] in each frame, thus allowing a frame-by-frame construction of a composite, superresolved image of a collection of densely packed molecules. Another, more direct approach uses computational image processing with *a priori* constraints under sufficiently high pixel brightness [5–10].

The covariance matrix, $V_\theta[\mathcal{O},\check{\theta}]$, for the unbiased estimator, $\check{\theta}$, of a set of quantities, $\theta \overset{\text{def}}{=} \{\theta_p | p = 1,\ldots,P\}$, parametrizing the density operator, $\hat{\rho}_\theta$, of a system is bounded below by the inverse of the quantum Fisher information (QFI) matrix [11–15], namely the quantum Cramér-Rao bound (QCRB),

$$V_\theta[\mathcal{O},\check{\theta}] \geq \mathbf{J}_\theta^{-1}[\mathcal{O}] \geq \mathbf{H}_\theta^{-1}, \tag{1}$$

in which $\mathcal{O} = \{\hat{O}(x)|x \in \mathcal{X}\}$ defines a positive-operator valued measure (POVM) of non-negative operators defined on a data set $\mathcal{X}$ and that sum to the identity operator, $\hat{I}$. The classical FI matrix, $\mathbf{J}_\theta[\mathcal{O}]$, is defined [16,17] in terms of the probability distribution (PD) of the POVM, $P_O(x;\theta) = \mathrm{Tr}[\hat{\rho}_\theta \hat{O}(x)]$, as

$$\mathbf{J}_\theta[\mathcal{O}] = \mathbb{E}_O(\nabla_\theta \ln P_O(x;\theta) \nabla_\theta^T \ln P_O(x;\theta)), \tag{2}$$

in which $\nabla_\theta \ln P$ is a column vector representing the gradient taken relative to θ, the superscript T denotes matrix transpose, and $\mathbb{E}_O$ the statistical expectation of its argument over the PD. The inverse of the classical FI is the classical Cramér-Rao lower bound (CRB).

Tsang *et al.* [18] proved that pair separation can achieve QCRB in one dimension with classical wave-front projections. This has been generalized to a thermal source pair of the same average but otherwise indefinite strength [19], to a source pair in an arbitrary quantum state [20], to homodyne and heterodyne detection [21], and to two dimensions [22], and experimentally verified by a number of groups [23–26]. For an imager with a one-dimensional Gaussian point-spread function (PSF), it is the Hermite Gaussian (HG) basis [18] that perfectly achieves QCRB, which turns out to be independent of the pair separation. By contrast, the conventional image-based approach entails a quadratic dependence of FI on the separation. This critical difference implies dramatically different inverse-square vs inverse-quartic power-law scalings of the minimum photon number needed to resolve the pair as a function of their separation using these two approaches.

Here we treat the problem of estimating the full three-dimensional (3D) separation vector for a pair of incoherent, equally bright point sources, when the pair centroid is known and an imager with a circular aperture is used [27]. We first calculate the 3×3 QFI matrix with respect to (w.r.t.) the three components of the pair separation vector, and show it to be diagonal and independent of the latter. We also show that QFI is in fact the same as that for localizing a single point emitter in 3D [28]. We then discuss projective-measurement protocols that can achieve QCRB in two special cases of vanishing axial and lateral separations. We finally present simulations of an experimental proposal to achieve quantum-limited 3D pair separation.

A photon emitted by an incoherent pair of equally bright point sources and passing through an imaging aperture is described by the density operator,

$$\hat{\rho} = \frac{1}{2}(|K_+\rangle\langle K_+| + |K_-\rangle\langle K_-|), \tag{3}$$

in which $|K_\pm\rangle$ are pure one-photon states passing through the aperture, corresponding to individual emissions by the two sources located at 3D positions, $\pm(\mathbf{r}_\perp, r_z)$, w.r.t. their centroid. The corresponding normalized transverse and axial semiseparations, $\boldsymbol{l}_\perp$, l_z, are defined as

$$\boldsymbol{l}_\perp = \mathbf{r}_\perp/\sigma_0, \qquad l_z = r_z/\zeta_0, \tag{4}$$

where $\sigma_0 = \lambda z_O/R$ and $\zeta_0 = \lambda z_O^2/R^2$ denote the characteristic transverse and axial resolution scales [29] for an aperture of radius R, optical wavelength λ, and distance z_O from the aperture of the pair centroid, the latter taken to be at the on-axis, in-focus position w.r.t. the aperture.

The coordinate representations, $\langle \mathbf{s}|K_\pm\rangle$, of these states are the image-plane amplitude PSFs. Their momentum-space representations are the wave functions in the exit pupil of the imager [29],

$$\langle \mathbf{u}|K_\pm\rangle = \exp(\pm i\phi_0)P(\mathbf{u})\exp[\mp i(2\pi \boldsymbol{l}_\perp \cdot \mathbf{u} + \pi l_z u^2)], \tag{5}$$

in which the linear and quadratic phases of each wave function represent, respectively, its tilt and curvature due to the off-axis, defocused location of the corresponding source, and $P(\mathbf{u})$ denotes a general aperture function. For a clear aperture, $P(\mathbf{u})$ is simply $1/\sqrt{\pi}$ times its indicator function, corresponding to the Airy PSF, while in its Gaussian form, it yields the Gaussian PSF. More generally, $P(\mathbf{u})$ need only obey the normalization condition,

$$\int d^2u |P(\mathbf{u})|^2 = 1, \tag{6}$$

which follows from requiring $\langle K_\pm|K_\pm\rangle = 1$.

The two nonzero eigenvalues, $e_\pm$, and the associated orthonormal eigenstates, $|e_\pm\rangle$, of $\hat{\rho}$ given by Eq. (3) are

$$e_\pm = (1 \pm \Delta)/2; \quad |e_\pm\rangle = [2(1 \pm \Delta)]^{-1/2}(|K_+\rangle \pm |K_-\rangle), \tag{7}$$

where Δ is the inner product, $\Delta = \langle K_-|K_+\rangle$, which we render real and positive by a proper choice of the phase constant, ϕ_0.

The QFI matrix has elements, $\mathrm{Re}H_{\mu\nu}$, where Re denotes the real part and $H_{\mu\nu} \overset{\text{def}}{=} \mathrm{Tr}(\hat{\rho}\hat{L}_\mu\hat{L}_\nu)$ can be expressed [30] in the eigenbasis of $\hat{\rho}$ as

$$H_{\mu\nu} = \sum_{i\in\mathcal{R}}\sum_j \frac{4e_i}{(e_i+e_j)^2}\langle e_i|\partial_\mu\hat{\rho}|e_j\rangle\langle e_j|\partial_\nu\hat{\rho}|e_i\rangle, \tag{8}$$

in which $\hat{L}_\mu$ is the symmetric logarithmic derivative (SLD) of $\hat{\rho}$ w.r.t. parameter l_μ, for brevity we denote $\partial\hat{\rho}/\partial l_\mu$ as $\partial_\mu\hat{\rho}$, and $\mathcal{R}$ denotes the set of values of an index for the eigenstates that span the range space of $\hat{\rho}$.

By decomposing the j sum into a sum over the range space of $\hat{\rho}$ and another over its null space, $j \notin \mathcal{R}$ for which $e_j = 0$, we may evaluate the latter sum via the completeness relation,

$$\sum_{j\notin\mathcal{R}}|e_j\rangle\langle e_j| = \hat{I} - \sum_{j\in\mathcal{R}}|e_j\rangle\langle e_j|.$$

We may thus express $H_{\mu\nu}$ in Eq. (8) as

$$H_{\mu\nu} = \sum_{i\in\mathcal{R}}\frac{4}{e_i}\langle e_i|\partial_\mu\hat{\rho}\partial_\nu\hat{\rho}|e_i\rangle + \sum_{i\in\mathcal{R}}\sum_{j\in\mathcal{R}}\left(\frac{4e_i}{(e_i+e_j)^2} - \frac{4}{e_i}\right)\langle e_i|\partial_\mu\hat{\rho}|e_j\rangle\langle e_j|\partial_\nu\hat{\rho}|e_i\rangle. \tag{9}$$

For the present problem for which $\mathcal{R} = \{+,-\}$, we may simplify the derivatives in Eq. (9) by means of the eigenvector identity, $\partial_\mu[(\hat{\rho} - e_i\hat{I})|e_i\rangle] = 0$, and thus express $H_{\mu\nu}$ as [30]

$$H_{\mu\nu} = \sum_{i=\pm}\frac{1}{e_i}\partial_\mu e_i\partial_\nu e_i + 4\sum_{i=\pm}\frac{1}{e_i}(\partial_\mu\langle e_i|)(\hat{\rho} - e_i\hat{I})^2\partial_\nu|e_i\rangle + 4\Delta^2\sum_{i\neq j}\left(\frac{1}{e_i} - e_i\right)\langle e_i|\partial_\mu|e_j\rangle\langle e_j|\partial_\nu|e_i\rangle, \tag{10}$$

in which we used the identities $e_+ + e_- = 1$ and $e_+ - e_- = \Delta$. The first sum in Eq. (10) may be regarded as the classical part of QFI, the real part of the second sum the contribution of quantum fluctuations of the photon state to QFI, and the real part of the final sum an additional contribution from the pair cross-coherence, $\Delta \neq 0$.

By evaluating the various state derivatives in Eq. (10), we may reduce it further [30] to the form,

$$H_{\mu\nu} = 4[(\partial_\mu\langle K_+|)\partial_\nu|K_+\rangle + \langle K_+|\partial_\mu|K_+\rangle\langle K_+|\partial_\nu|K_+\rangle]. \tag{11}$$

By using Eq. (5) for $\langle \mathbf{u}|K_+\rangle$, we may evaluate Eq. (11) in terms of the gradient of the phase function,

$$\Psi(\mathbf{u};\boldsymbol{l}) = 2\pi\boldsymbol{l}_\perp\cdot\mathbf{u} + \pi l_z u^2, \tag{12}$$

independently of ϕ_0 as

$$H_{\mu\nu} = 4[\langle\partial_\mu\Psi\partial_\nu\Psi\rangle - \langle\partial_\mu\Psi\rangle\langle\partial_\nu\Psi\rangle], \tag{13}$$

where angular brackets now denote averages over the modulus squared aperture function, $|P(\mathbf{u})|^2$.

The form of QFI found in Eq. (13) underscores the fundamental role of the correlations of the wave-front gradient in the aperture in controlling the error of estimation of the pair separation. For a clear circular aperture, to

which we restrict attention in the rest of the Letter and for which $|P(\mathbf{u})|^2$ is $1/\pi$ times its indicator function, simple integrations yield the following averages:

$$\langle u_i\rangle = 0; \quad \langle u_i u_j\rangle = \frac{\delta_{ij}}{4};$$
$$\langle u^2\rangle = \frac{1}{2}; \quad \langle u^4\rangle = \frac{1}{3}; \quad i,j = x,y, \tag{14}$$

and thus the following purely diagonal form of the per-photon 3D QFI matrix:

$$\mathbf{H}(l_x,l_y,l_z) = \begin{pmatrix} 4\pi^2 & 0 & 0 \\ 0 & 4\pi^2 & 0 \\ 0 & 0 & \frac{\pi^2}{3} \end{pmatrix}. \tag{15}$$

The reality and diagonal character of $H_{\mu\nu}$ provide necessary and sufficient achievability conditions for the simultaneous estimation of the three separation coordinates in the asymptotic limit, with collective measurements involving an arbitrarily large number of copies of the state [31]. For special cases, however, we will show presently that QCRB can be realized without the need for collective measurements.

We next show that QFI for localizing a single source, say the one located at $+(\boldsymbol{l}_\perp, l_z)$, is identical to that we have just obtained for 3D pair separation. For this problem, only the middle term in Eq. (10) contributes, since $\hat{\rho} = |K_+\rangle\langle K_+|$ has a single fixed nonzero eigenvalue, $e_+ = 1$, with eigenstate $|e_+\rangle = |K_+\rangle$, and $(\hat{\rho} - \hat{I})^2 = \hat{I} - |K_+\rangle\langle K_+|$. In view of these relations and normalization, $\langle K_+|K_+\rangle = 1$, which requires that $(\partial_\mu\langle K_+|)|K_+\rangle = -\langle K_+|\partial_\mu|K_+\rangle$, the resulting QFI becomes identical to Eq. (11) for QFI for source-pair separation. The equality of the QFI matrices for source localization and pair separation shows that the general problem is one of estimating the photon state, independent of the nature of its emitter.

The 3D source-localization QFI has been calculated directly from the definition of SLD of the density operator for a pure state in Ref. [28], but unlike that problem estimating the separation between incoherent sources requires use of a mixed state and thus the more general Eq. (9) for QFI. For two incoherent sources, Eq. (9) simplifies to Eq. (10), from which one can go further and consider QFI limited error bounds on joint localization and separation of the two [32].

QCRB is achievable via orthonormal wave-front projections in two special cases. For sources in the same transverse plane, for which $l_z = 0$, consider an orthonormal basis, $\mathcal{A} = \{A_{mn}(\mathbf{u})|m,n \in \mathbb{Z}\}$, of states in the aperture plane obeying the condition, $|\langle K_+|A_{mn}\rangle| = |\langle K_-|A_{mn}\rangle|$, $\forall\ m,n$. Since $\langle \mathbf{u}|K_+\rangle = \langle \mathbf{u}|K_-\rangle^*$, this condition is met by *any* real basis. The probability $P^{(A)}_{mn}$, which is equal to $\langle A_{mn}|\hat{\rho}|A_{mn}\rangle$, may then be written as $P^{(A)}_{mn} = |\langle K_+|A_{mn}\rangle|^2$, from which follow the FI matrix elements,

$$J_{\mu\nu}[\mathcal{A}] = \sum_{m,n} \frac{\partial_\mu P^{(A)}_{mn}\partial_\nu P^{(A)}_{mn}}{P^{(A)}_{mn}}$$
$$= 4\sum_{m,n} \partial_\mu|\langle A_{mn}|K_+\rangle|\partial_\nu|\langle A_{mn}|K_+\rangle|. \tag{16}$$

If we assume further that the phases of $\langle K_+|A_{mn}\rangle$ are independent of $\boldsymbol{l}_\perp$, then Eq. (16) simplifies to

$$J_{\mu\nu}[\mathcal{A}] = 4\sum_{m,n} (\partial_\mu\langle K_+|)|A_{mn}\rangle\langle A_{mn}|\partial_\nu|K_+\rangle$$
$$= 4(\partial_\mu\langle K_+|)\partial_\nu|K_+\rangle, \tag{17}$$

with the second equality following from the completeness relation, $\sum_{m,n}|A_{mn}\rangle\langle A_{mn}| = \hat{I}$. For $\mu,\ \nu = x,\ y$, $J_{\mu\nu}[\mathcal{A}]$ matches QFI in Eq. (11) since for the choice, $\phi_0 = 0$, that we make to render the phases of $\langle K_+|A_{mn}\rangle$ independent of $\boldsymbol{l}_\perp$, $\langle K_+|\partial_\mu|K_+\rangle$ vanishes identically for any inversion symmetric aperture.

The orthonormal sine-cosine Fourier basis states in polar coordinates, (u,ϕ),

$$\mathrm{CC}_{mn}(\mathbf{u}) = \sqrt{\frac{c_m c_n}{\pi}}\cos(2\pi m u^2)\cos n\phi, \quad m,n = 0,1,\ldots,$$
$$\mathrm{CS}_{mn}(\mathbf{u}) = \sqrt{\frac{c_m c_n}{\pi}}\cos(2\pi m u^2)\sin n\phi, \quad m = 0,1,\ldots, \quad n = 1,2,\ldots,$$
$$\mathrm{SC}_{mn}(\mathbf{u}) = \sqrt{\frac{c_m c_n}{\pi}}\sin(2\pi m u^2)\cos n\phi, \quad m = 1,2,\ldots, \quad n = 0,1,\ldots,$$
$$\mathrm{SS}_{mn}(\mathbf{u}) = \sqrt{\frac{c_m c_n}{\pi}}\sin(2\pi m u^2)\sin n\phi, \quad m,n = 1,2,\ldots, \tag{18}$$

with $c_n = 2 - \delta_{n0}$, constitute one such basis that achieves QFI for the case of pure transverse pair separation as their overlap integrals with the photon wave front of each source can be readily shown [30] to have phases that are independent of that separation.

For the source pair being on the optical axis, i.e., $l_\perp = 0$, only the $n = 0$ subset of the sine-cosine basis, as we need no angular localization, achieves QCRB w.r.t. l_z, as we show next. The relevant probability amplitudes are

$$\langle A_{m0}|K_+\rangle = \frac{1}{\sqrt{\pi}}\int_0^1 du u \exp(-i\pi l_z u^2)A_{m0}(u),$$
$$= \frac{1}{2\sqrt{\pi}}\exp\left(-i\pi\frac{l_z}{2}\right)\int_{-1/2}^{1/2} dv \cos(\pi l_z v)A_{m0}(\sqrt{v+1/2}), \tag{19}$$

with $A = \mathrm{CC}$, SC. We used the variable transformation, $v = u^2 - 1/2$, followed by a symmetrization of the

resulting integrand to reach the second equality in Eq. (19) that involves a purely real integral. It thus follows that up to a sign $|\langle A_{m0}|K_+\rangle| = \exp(i\pi l_z/2)\langle A_{m0}|K_+\rangle$, which allows us, analogously to Eq. (16) with $\mu = \nu = z$, to express FI w.r.t. l_z as

$$\begin{aligned} J_{zz}[\mathcal{A}] &= 4\sum_m |\partial_z|\langle A_{m0}|K_+\rangle\|^2 \\ &= 4\sum_m [\partial_z(\langle K_+|)|A_{m0}\rangle - i(\pi/2)\langle K_+|A_{m0}\rangle] \times [\langle A_{m0}|\partial_z|K_+\rangle + i(\pi/2)\langle A_{m0}|K_+\rangle] \\ &= 4[\partial_z(\langle K_+|)|\partial_z|K_+\rangle - i(\pi/2)\langle K_+|\partial_z|K_+\rangle + i(\pi/2)(\partial_z|K_+\rangle)|K_+\rangle + (\pi/2)^2] \\ &= 4[\partial_z(\langle K_+|)|\partial_z|K_+\rangle - \pi^2/4] \\ &= 4[\partial_z(\langle K_+|)|\partial_z|K_+\rangle + \langle K_+|\partial_z|K_+\rangle^2], \end{aligned} \tag{20}$$

in which we used the completeness of the $|A_{m0}\rangle$ states over the aperture for ϕ-invariant wave functions like $\langle \mathbf{u}|K_+\rangle$, which is characteristic of an axially separated source pair, and relations, $\langle K_+|\partial_z|K_+\rangle = (\partial_z\langle K_+|)|K_+\rangle^* = -i\pi\langle u^2\rangle = -i\pi/2$, to derive the various expressions. We see from Eq. (11) that the $\{A_{m0}|A = \mathrm{CC}, \mathrm{SC}, m = 0, 1, \ldots\}$ basis achieves QFI w.r.t. l_z for an axially separated source pair. More generally, any real basis of orthonormal projections, $\{|B_m\rangle\}$, for which the equality, $|\langle B_m|K_+\rangle| = |\langle B_m|K_-\rangle|$, certainly holds, will achieve QFI.

Projections that are well matched to the linear tilt and quadratic defocus parts of the aperture phase function, $\Psi(\mathbf{u})$, given by Eq. (12), can achieve full 3D QFI in the limit of small separations, $l_\perp, l_z \ll 1$. One need merely use a few such projections, as noted in Ref. [18], to attain quantum-limited estimation variance in this limit. In the 3D case, we consider aperture-plane wave-front projections into low-order orthonormal Zernike basis functions [33], $\{Z_n, n = 1, 2, \ldots, N\}$, with $N \sim 4$–7. Here we only discuss projections into the first four Zernikes,

$$\begin{aligned} Z_1 &= \frac{1}{\sqrt{\pi}}, \qquad Z_2 = \frac{2}{\sqrt{\pi}} u\cos\phi, \\ Z_3 &= \frac{2}{\sqrt{\pi}} u\sin\phi, \qquad Z_4 = \sqrt{\frac{3}{\pi}}(2u^2 - 1). \end{aligned} \tag{21}$$

The second and third of these correlate perfectly, respectively, with the tilt phases corresponding to the x and y components of the transverse separation vector, $\boldsymbol{l}_\perp$, and may thus be regarded as matched filters [34] for the latter. By contrast, the first and last are only partially matched to the quadratic pupil phase corresponding to the axial separation, l_z, with their probabilities remaining finite when $l_z \to 0$. The imperfect match of the latter with a single projection mode causes striking differences, as we shall see, in the estimation error bounds that are achievable in the limit of vanishing separation.

We now prove these assertions by evaluating [30] the mode-projection probabilities, $P_n = \langle Z_n|\hat{\rho}|Z_n\rangle$, for $l_\perp$, $l_z \ll 1$,

$$P_n = \begin{cases} 1 - \pi^2(l_\perp^2 + l_z^2/12) + O(l_\perp^4, l_z^4) & n = 1 \\ \pi^2 l_x^2[1 + O(l_\perp^2, l_z^2)] & n = 2 \\ \pi^2 l_y^2[1 + O(l_\perp^2, l_z^2)] & n = 3 \\ \pi^2 l_z^2/12 + O(l_\perp^4, l_z^2 l_\perp^2, l_z^4) & n = 4 \end{cases}. \tag{22}$$

Since $(\partial_x P_2)^2/P_2 = (\partial_y P_3)^2/P_3 = 4\pi^2[1 + O(l_z^2)]$, we see that each reaches QFI in the limit $l_z \to 0$. By contrast, the Z_4 projection contributes to FI w.r.t. l_z the term, $(\partial_z P_4)^2/P_4$, which is of form $(\pi^2/3)(l_z^2/\{l_z^2[1 + O(l_\perp^2)] + O(l_\perp^4)\})$ and vanishes in the limit $l_z \to 0$ if $l_\perp \neq 0$. The same form implies, however, that for $l_\perp \ll 1$, FI as a function of l_z rises to a value comparable to the QFI, $\pi^2/3$ over an interval of order $l_\perp^2$. All other contributions to the various matrix elements of FI are negligibly small in the limit of vanishing l, so the inverse of the diagonal elements of FI determine the corresponding CRBs to the most significant order in l.

One can perform wave-front projections by digital holography [23]. Specifically, consider encoding the sum, $\sum_{n=1}^N Z_n(\mathbf{u})\cos(\mathbf{q}_n \cdot \mathbf{u})$, as the distribution of the amplitude transmittance of a plate, with negative values in the sum realized by a π phase retardation. Let the imaging wave front, which is an incoherent superposition of the photon wave functions $\langle \mathbf{u}|K_\pm\rangle$ and carries M photons, be incident on such a plate that is placed in the aperture (or a conjugate plane thereof), and then optically focused on a sensor. The M photons will divide into N pairs of oppositely located spots, with the nth pair of spots corresponding to an obliquely propagating wave pair that carries the Z_n projection of the incident wave front along the spherical-angle pair, $(\theta_n, \pm\phi_n)$, with $\theta_n = \sin^{-1}(q_n/k)$ and $\phi_n = \tan^{-1}(q_{ny}/q_{nx})$. The numbers of photons detected at the central pixels of the spots taken pairwise furnish estimates of the probabilities of the wave front being in the corresponding modes. The remaining photons that are not detected provide an estimate of the wave front being in the remaining states of a complete basis of which the subset, $\{Z_n, n = 1, \ldots, N\}$, defines the observed states.

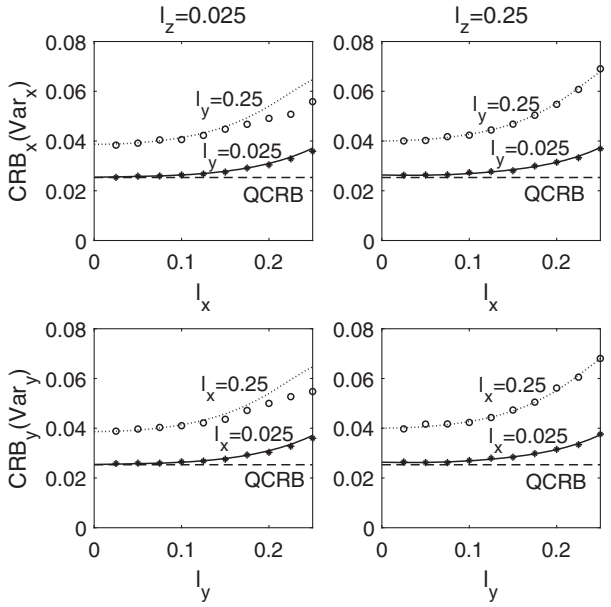

FIG. 1. Plots of CRBs w.r.t. l_x for $l_y = 0.025$ (lower curve) and $l_y = 0.25$ (upper curve) and for $l_z = 0.025$ (left panels) and $l_z = 0.25$ (right panels). The roles of l_x and l_y are interchanged in the bottom panels. Estimation variances obtained from simulation are shown by different marker symbols.

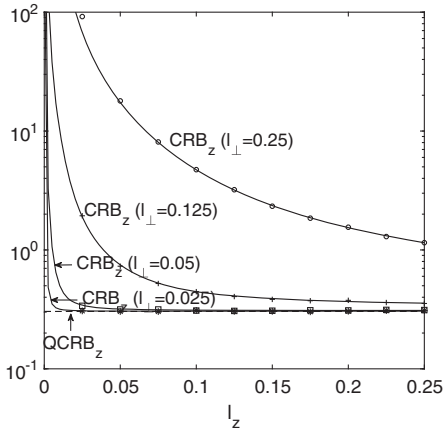

FIG. 2. Plots of CRB w.r.t. l_z, for four different values of $l_\perp$, namely 0.025, 0.05, 0.125, and 0.25. Simulated estimation variances are shown by different marker symbols.

The probability of detecting $m_1, \ldots, m_N$ photons in the N projective channels is given by the multinomial (MN) distribution [30],

$$\mathrm{Prob}(\bar{m}, \{m_n\}|\{P_n\}) = M! \frac{\bar{P}^{\bar{m}}}{\bar{m}!} \prod_{n=1}^{N} \frac{(P_n)^{m_n}}{m_n!}, \qquad (23)$$

in which $\bar{m} = M - \sum_{n=1}^{N} m_n$ and $\bar{P} = 1 - \sum_{n=1}^{N} P_n$ are, respectively, the number and probability of undetected photons. Expressing the P_n in terms of the separation coordinates, l_x, l_y, l_z, we performed their maximum-likelihood (ML) estimation by numerically minimizing $-\ln \mathrm{Prob}$ over those coordinates using Matlab's *fminunc* minimizer, which we started with an initial guess of $l_x = l_y = l_z = 1/4$, for a number of separations, 20 000 frames of noisy data, each with $M = 10^6$ photons and generated using Matlab's *mnrnd* code.

We plot in Fig. 1 the per-photon CRBs w.r.t. l_x (top panels) and l_y (bottom panels) for two different values of their axial separation, $l_z = 0.025$ (left panels) and 0.25 (right panels). For each plot, we considered two different values, 0.025 and 0.25, of the other transverse coordinate, shown via the two different curves in each figure. Note that CRB w.r.t. each transverse-separation coordinate increases with increasing value of the other coordinate due to a cross-talk between the two transverse coordinates. Changing the longitudinal separation, however, has a less pronounced effect on those curves. As the pair separation increases, using only the first four Zernikes is insufficient to estimate $\boldsymbol{l}_\perp$, which accounts in part for the rising CRB curves.The discrete points identified by marker symbols are the results of the sample-based variance (per photon) of the ML estimate of the separation coordinates that we obtained in our numerical simulations. Note that the results of simulation are consistently lower than the corresponding CRB curves, which is most discernible in the left panels ($l_z = 0.025$). This is because the ML estimates of the separation coordinates are biased, particularly that for l_z, and standard CRBs do not provide the correct lower bounds without including bias-gradient based modifications [16,17].

In Fig. 2 we plot the per-photon CRBs w.r.t. l_z for four different values of $l_\perp$. We observe divergent behavior as l_z approaches zero, corresponding to the vanishing of $J_{zz}[Z]$ whenever $l_\perp \neq 0$ that we noted earlier. This behavior is quite in contrast with the rather muted dependence on l_z which we observed in Fig. 1 for the CRBs w.r.t. $\boldsymbol{l}_\perp$. The cross-talk between the uncertainties in simultaneously estimating the three pair-separation coordinates, which is inherently present in the small set of Zernike projections, increases the CRB for l_z estimation as $l_\perp$ increases. The simulated values of the variance of the estimator of l_z, indicated by marker symbols, agree well with the theoretical CRB values.

This Letter has treated the fundamental error in estimating the full 3D separation vector for a source pair by calculating the corresponding QFI and proposing specific projection bases for which QFI is attainable. Simulations using the Zernike basis confirm our theoretical assertions.

The work was partially supported by the US Air Force Office of Scientific Research under Grant No. FA9550-15-1-0286. The authors are grateful to G. Adesso for pointing out his group's very recent work [35] on the simultaneous estimation of the angular and axial separations as well as the coordinates of the centroid of an incoherent source pair located in a single meridional plane.

*Also at School of Physics and Astronomy, University of Minnesota, Minneapolis, Minnesota 55455, USA.
sprasad@unm.edu

[1] L. Rayleigh, XXXI. Investigations in optics, with special reference to the spectroscope, Philos. Mag. **8**, 261 (1879).
[2] W. E. Moerner and L. Kador, Optical Detection and Spectroscopy of Single Molecules in a Solid, Phys. Rev. Lett. **62**, 2535 (1989).
[3] S. W. Hell and J. Wichmann, Breaking the diffraction resolution limit by stimulated emission: Stimulated-emission-depletion fluorescence microscopy, Opt. Lett. **19**, 780 (1994).
[4] E. Betzig, Proposed method for molecular optical imaging, Opt. Lett. **20**, 237 (1995).
[5] C. Rushforth and R. Harris, Restoration, resolution, and noise, J. Opt. Soc. Am. **58**, 539 (1968).
[6] M. Bertero and C. De Mol, Superresolution by data inversion, Prog. Opt. **36**, 129 (1996).
[7] L. Lucy, Statistical limits to superresolution, Astron. Astrophys. **261**, 706 (1992).
[8] M. Shahram and P. Milanfar, Imaging below the diffraction limit: A statistical analysis, IEEE Trans. Image Process. **13**, 677 (2004).
[9] S. Ram, E. Sally Ward, and R. Ober, Beyond Rayleigh's criterion: A resolution measure with application to single-molecule microscopy, Proc. Natl. Acad. Sci. U.S.A. **103**, 4457 (2006).
[10] S. Prasad, Asymptotics of Bayesian error probability and 2D pair superresolution, Opt. Express **22**, 16029 (2014).
[11] C. Helstrom, *Quantum Detection and Estimation Theory* (Academic Press, New York, 1976), Vol. 123.
[12] S. L. Braunstein and C. M. Caves, Statistical Distance and the Geometry of Quantum States, Phys. Rev. Lett. **72**, 3439 (1994).
[13] M. Paris, Quantum estimation for quantum technology, Int. J. Quantum. Inform. **07**, 125 (2009).
[14] M. Szczykulska, T. Baumgraz, and A. Dutta, Multi-parameter quantum metrology, Adv. Phys. X **1**, 621 (2016).
[15] D. Safranek, Simple expression for the quantum Fisher information matrix, Phys. Rev. A **97**, 042322 (2018).
[16] H. Van Trees, *Detection, Estimation, and Modulation Theory, Part I* (Wiley, New York, 1968).
[17] S. Kay, *Fundamentals of Statistical Signal Processing: I. Estimation Theory* (Prentice Hall, New Jersey, 1993).
[18] M. Tsang, R. Nair, and X.-M. Lu, Quantum Theory of Superresolution for Two Incoherent Optical Point Sources, Phys. Rev. X **6**, 031033 (2016).
[19] R. Nair and M. Tsang, Far-Field Superresolution of Thermal Electromagnetic Sources at the Quantum Limit, Phys. Rev. Lett. **117**, 190801 (2016).
[20] C. Lupo and S. Pirandola, Ultimate Precision Bound of Quantum and Sub-Wavelength Imaging, Phys. Rev. Lett. **117**, 190802 (2016).
[21] F. Yang, R. Nair, M. Tsang, C. Simon, and A. I. Lvovsky, Fisher information for far-field linear optical superresolution via homodyne or heterodyne detection in a higher-order local oscillator mode, Phys. Rev. A **96**, 063829 (2017).
[22] S. Z. Ang, R. Nair, and M. Tsang, Quantum limit for two-dimensional resolution of two incoherent optical point sources, Phys. Rev. A **95**, 063847 (2017).
[23] M. Paúr, B. Stoklasa, Z. Hradil, L. Sanchez-Soto, and J. Rehacek, Achieving the ultimate optical resolution, Optica **3**, 1144 (2016).
[24] Z. S. Tang, K. Durak, and A. Ling, Fault-tolerant and finite-error localization for point emitters within the diffraction limit, Opt. Express **24**, 22004 (2016).
[25] F. Yang, A. Taschilina, E. S. Moiseev, C. Simon, and A. I. Lvovsky, Far-field linear optical superresolution via heterodyne detection in a higher-order local oscillator mode, Optica **3**, 1148 (2016).
[26] W. K. Tham, H. Ferretti, and A. M. Steinberg, Beating Rayleigh's Curse by Imaging Using Phase Information, Phys. Rev. Lett. **118**, 070801 (2017).
[27] Preliminary results appeared in S. Prasad and Z. Yu, Quantum theory of three-dimensional superresolution using rotating-PSF imagery, in *Proceedings of Advanced Maui Optical and Space Surveillance (AMOS) Technologies Conference* (Maui Economic Development Board, 2017), https://amostech.com/TechnicalPapers/2017/Adaptive-Optics_Imaging/Prasad.pdf.
[28] M. P. Backlund, Y. Shechtman, and R. L. Walsworth, Fundamental Precision Bounds for Three-Dimensional Optical Localization Microscopy with Poisson Statistics, Phys. Rev. Lett. **121**, 023904 (2018).
[29] J. Goodman, *Introduction to Fourier Optics*, 4th ed. (Freeman, New York, 2017).
[30] See Supplemental Material at http://link.aps.org/supplemental/10.1103/PhysRevLett.121.180504 for a derivation of certain QFI expressions, useful properties of the sine, cosine, and Zernike projections, and a derivation of the likelihood function for the photon counts observed in different projection channels.
[31] S. Ragy, M. Jarzyna, and R. Demkowicz-Dobrzański, Compatibility in multiparameter quantum metrology, Phys. Rev. A **94**, 052108 (2016).
[32] S. Prasad and Z. Yu, Quantum limited super-localization and super-resolution of a source pair in three dimensions, arXiv:1807.09853 [Phys. Rev. A (to be published)].
[33] R. Noll, Zernike polynomials and atmospheric turbulence, J. Opt. Soc. Am. **66**, 207 (1976).
[34] G. Turin, An introduction to matched filters, IRE Trans. Inf. Theory **6**, 311 (1960).
[35] C. Napoli, T. Tufarelli, S. Piano, R. Leach, and G. Adesso, Towards Superresolution Surface Metrology: Quantum Estimation of Angular and Axial Separations, arXiv:1805.04116 [Phys. Rev. Lett. (to be published)].